Published in final edited form as:
Environ Sci Technol. 2005 September 15; 39(18): 7012–7019.

Molecular Tracers of Saturated and Polycyclic Aromatic Hydrocarbon Inputs into Central Park Lake, New York City

BEIZHAN YAN[†,§], **TEOFILO A. ABRAJANO**[*,†], **RICHARD F. BOPP**[†], **DAMON A. CHAKY**[‡], **LUCILLE A. BENEDICT**[†], and **STEVEN N. CHILLRUD**[‡]
Department of Earth and Environmental Sciences, Rensselaer Polytechnic Institute, Troy, New York 12180, and Geochemistry Division, Lamont-Doherty Earth Observatory of Columbia University, Palisades, New York 10964

Abstract

Saturated hydrocarbons (SH) and polycyclic aromatic hydrocarbons (PAHs) have been quantified in a sediment core obtained from Central Park Lake, New York City. Radionuclides ^{210}Pb and ^{137}Cs were used to assign approximate dates to each individual section in the core. The dating profile based on ^{210}Pb matches very well with the time constraints provided by ^{137}Cs. Radionuclide-derived depositional dates are consistent with temporal information from the petroleum-indicator ratio U/R [the ratio of unresolved complex mixture (UCM) to saturated hydrocarbons in the aliphatic fraction] and the history of fuel use in the NYC area. Ratios of 1,7-dimethylphenanthrane (DMP) to 1,7-DMP plus 2,6-DMP [1,7/(1,7 + 2,6)-DMP], retene to retene plus chrysene [Ret/(Ret + Chy)], and fluoranthene to fluoranthene plus pyrene [Fl/(Fl + Py)] provide additional source discrimination throughout the core. Results show that the ratio U/R is sensitive to petroleum inputs and Ret/(Ret + Chy) is responsive to contributions from softwood combustion, whereas both Fl/(Fl + Py) and 1,7/(1,7 + 2,6)-DMP can be used to discriminate among wood, coal, and petroleum combustion sources. Combined use of these ratios suggests that in New York City, wood combustion dominated 100 years ago, with a shift to coal combustion occurring from the 1900s to the 1950s. Petroleum use began around the 1920s and has dominated since the 1940s.

Introduction

Early in 1933 benzo[*a*]pyrene (BaP), a high molecular weight (HMW) compound of the polycyclic aromatic hydrocarbons (PAHs), was first isolated from coal tar in England (1). Great attention has been given to this important class of organic contaminants since then due to the toxicity of their lower molecular weight (LMW) components and the carcinogenicity and mutagenicity of HMW components (2). PAHs can be produced naturally or anthropogenically. In a highly urbanized area like New York City, natural biogenic sources (e.g. sedimentary early diagenetic processes) are a relatively minor contributor and can be neglected compared with important anthropogenic sources (3). Anthropogenic sources include pyrogenic sources, such as the incomplete combustion of fossil fuels (petroleum and coal) or biofuels (e.g. grass, trees, or duff) (4), and petrogenic sources, such as the direct release of these fossil fuels and the leakage of crankcase oil (5, 6).

[*]Corresponding author phone: (518) 276-6036; fax: (518) 276-2012; abrajt@rpi.edu.
[†]Rensselaer Polytechnic Institute.
[‡]Lamont-Doherty Earth Observatory of Columbia University.
[§]Current address: Department of Chemistry, University of Idaho at Idaho Falls, Idaho Falls, ID 83402.

Different PAH sources yield different molecular distribution patterns because of the variety of substrates, pathways, and conditions of PAH formation (2, 5, 7). For example, combustion-derived PAHs are predominately parental and HMW PAHs (4–6 ring), whereas petroleum-related PAHs are largely alkylated homologues and LMW compounds (2). In addition, ratios of some isomer pairs vary from source to source (8). For instance, fluoranthene and anthracene are preferentially produced during incomplete combustion relative to their corresponding isomers, pyrene and phenanthrene, respectively (5). On the basis of these differences, previous workers have employed various molecular ratios (Table 1) as PAH source indicators (8). Two ratios derived from compound groups, the fraction of 4–6 ring PAH relative to the total PAH (Ring456/TPAH) and the fraction of parental PAH relative to the total PAH [Par/(Par + Alkyl)], have been suggested and successfully applied as PAH source indicators (Table 1) (9).

The above ratios were initially proposed as a tool to distinguish petrogenic and pyrogenic PAH sources. However, studies have shown that pyrogenic sources are quantitatively the most dominant sources of PAHs in modern sediments (10). Pyrogenic PAHs can originate from many pyrolysis substrates, including wood, coal, and petroleum combustion (e.g., space heating and motor vehicle emissions). There have been many attempts to determine specific pyrogenic sources on the basis of PAH composition (11–13). For example, it has been observed that 1,7-dimethylphenanthrene (DMP) is preferentially produced in softwood combustion emissions, and 2,6-DMP is found with comparable concentrations in emissions from both fossil fuel and softwood combustion. The ratio of 1,7-dimethylphenanthrene (DMP) to 2,6-DMP in air particulate matter has been proposed and successfully used to distinguish softwood combustion from motor vehicle emissions (11). Another compound, retene (1-methyl-7-isopropylphenanthrene), has also been proposed as a “fingerprint” of softwood combustion (12). Researchers have identified relatively trace amounts of picene and hydropicene homologues compared with other 4- and 5-ring PAHs in emissions from coal combustion (14); however, the uniqueness of picene and hydropicene homologues for differentiating coal-derived from other PAH inputs has been called into question, since these picene-related compounds have been identified in diesel exhaust emissions as well (15).

Central Park Lake sediment cores have been used previously to investigate the history of atmospheric deposition of trace metals (16) and chlorinated organics (17) in New York City (NYC). The present study takes advantage of radionuclide-dated sediment cores from this previous work, which revealed ca. 130 years of history of sediment and contaminant deposition. This time period witnessed large changes in the predominant fuel type used in NYC. Historical trends in fuel use in NYC are derived from U.S. national data collected by the Energy Information Administration (EIA) (18). EIA data were scaled to NYC population trends (available at http://www.demographia.com/db-nyc2000.html) to provide quantitative historical estimates of fuel use in the NYC area. This fuel-use history can be used to evaluate the usefulness and limitations of various PAH source indicators (Table 1) and current widely applied saturated hydrocarbon (SH) indicators (e.g. U/R, the area ratio of unresolved “hump” to resolved peaks in a chromatogram). In a manuscript in preparation, estimation of SH and PAH depositional fluxes and a semi-quantitative estimate of the proportion of various combustion sources are developed from the more reliable source-indicator ratios identified in this paper.

Methods

Four push cores with similar lengths (50 ± 6 cm) were collected in January of 1996 from Central Park (CP) Lake located in the center of Manhattan. The lake history and surrounding environments have been described in another paper (16). Briefly, CP Lake was completed in the 1860s with a water surface area of approximately 7.1×10^4 m^2 and total drainage area of

about 7.0×10^5 m^2. Park roads cover 5.2×10^4 m^2 of the watershed, and road runoff drains into the lake via a series of six drainage pipes that include sediment traps designed to limit particulate inputs into the lake (16).

Two cores (CPE, CPF) were collected from the western basin of the lake and two cores (CPG, CPH) from the eastern basin of the lake. All cores were sliced into 2-cm sections soon after sampling. Sectioned samples were dried at 35 °C under a flow of air filtered through Florisil to minimize possible contamination from lab air. Dried samples were then ground and homogenized to fine powders with a mortar and pestle.

A detailed description of the dating methods has been reported previously (16). The activities of the particle-associated radionuclides ^{7}Be, ^{137}Cs, and unsupported ^{210}Pb ($^{210}Pb_{xs}$) were analyzed by γ spectrometry using a lithium-drifted germanium or intrinsic germanium detector. The short-lived nuclide ^{7}Be ($t_{1/2}$ = 53 days) is naturally created in the upper levels of the atmosphere through spallation of N_2 and O_2 by cosmic rays. The presence of 7Be in the top few centimeters of a sediment core is evidence of recent sedimentation. Depth profiles of ^{137}Cs provide two dateable horizons tied to the atmospheric testing of nuclear weapons: 1954, the beginning of measurable activities in sediments for global fallout, and 1963, the peak year of atmospheric testing. $^{210}Pb_{xs}$ activities were determined as described in Chillrud et al. (16).

Samples were Soxhlet-extracted overnight using dichloromethane (DCM), after which the extracts were concentrated to 0.5 mL under a gentle flow of N_2. Following alumina column cleanup to remove the more polar compounds, activated copper powder was added to remove elemental sulfur. The extracts were separated into two fractions using silica chromatography: the first fraction eluted with hexane and contained the low polarity saturated hydrocarbons and PCBs; the second fraction eluted with CH_2Cl_2 and contained more polar compounds such as PAHs and pesticides (19).

Aliphatic and aromatic hydrocarbons were identified by capillary gas chromatography with a mass spectrometer (GC–MS) detector. High-purity PAH standards were purchased from Accustandard, Chiron, and Supelco. Standards include normal saturated hydrocarbons from C_{13} to C_{35}, 16 EPA parent PAHs, some C_1–C_4 alkyl PAHs homologues, dibenzothiophene series, and retene. The quantification of both saturated and unsaturated fractions was carried out by GC flame ionization detector (FID) due to its high linearity for different PAH concentrations and its predictable decrease of area responses (peak area per nanogram of carbon) with retention times. Area responses were used for calibration of PAH compounds in analytical standards. For those compounds without available standards, area responses were interpolated from the trend of the area response vs retention time (r^2 = 0.97). GC FID analysis was performed on a Fisons Instruments 8000 series gas chromatograph, equipped with a Restek DB-5 capillary column (0.32 mm i.d., 60 m, 0.25 μm film thickness) and a Fisons EL980 FID electrometer. Mass spectrometry utilized a Shimadzu GCMS-QP5050 in selective ion mode.

To ensure data quality in the PAH analysis, over 5% of the total number of samples analyzed in our lab were extracted and analyzed more than once using different sample weights. The percent difference in calculated concentrations was ~9% for sample weights greater than 1 g. One in every 10 sample extracts was injected twice, providing duplicate chromatographic runs. The results showed that the measured total PAH with different sample volumes varied by less than 4% (20). For comparative purposes, some sediment samples that were also extracted and analyzed at RPI have been sent to the NYSDEC contract labs (Philip Analytical Services and Severn-Trent Labs). The molecular distributions and compound concentrations were quite similar among all three labs.

Although the two commercial labs reported somewhat different concentrations for a handful of principal PAHs (e.g., Pa, Fl, Py), our lab was well within the range of these commercial measurements.

Results and Discussion

Sediment Dating

Consistent depth profiles of radionuclides ^{137}Cs and ^{210}Pb were observed in all four collected cores (16). Aliquots of core CPF were used for this hydrocarbon study, since sediments from other CP cores have been largely consumed for other studies. For CPF, several time constraints can be assigned to specific sediment intervals: measurable ^{7}Be activities in the top section, indicating deposition within a year of collection (19), and mid-1960s and early 1950s time horizons based on the ^{137}Cs activity profile, corresponding to the depth intervals of 14–16 and 20–22 cm, respectively.

Both constant length and constant mass dating models were considered (17). A constant mass dating method based on ^{210}Pb gave results similar to that of Chillrud et al. (16) in their study of core CPH. Two different mass accumulation rates are suggested: a lower rate in the upper portion of CPF (0.07 g/cm^2/yr from 0 to 14 cm) and a higher rate below (0.12 g/cm^2/yr at >14 cm). In comparison, a constant length model results in an accumulation rate of ~0.44 cm/yr, based on the time constraints provided by ^{7}Be (surface = 1996) and ^{137}Cs activities (peak activity at 14–16 cm in 1963; deepest detectable activity at 20–22 cm in 1954). An extrapolation of the 0.44 cm/yr linear accumulation rate through the rest of the core gives a very good match with the dates derived from the ^{210}Pb mass accumulation model. ^{210}Pb- and ^{137}Cs-derived depositional ages differ by ~10 years in non-^{137}Cs-bearing sections of the core, and are in excellent agreement (±3 years) over the last ~50 years (Figure 1). Similar to what was observed in core CPH (16), the bottom section of core CPF (52–55.5 cm) had a bulk density similar to that of CP soils and substantially greater than the bulk densities observed in all overlying sections; consequently, it was disregarded for organic contaminant analysis (Table 1). The two dating models for CPF are consistent with an age for the penultimate section of several decades prior to 1900, consistent with the time of creation of the lake. In the following discussion, any specific dates mentioned are from the ^{210}Pb mass accumulation dating model for CPF.

Temporal Trends of TSH and SH Indicators

Concentrations of the total of saturated hydrocarbon fraction (TSH), which includes resolved hydrocarbon peaks and the unresolved complex mixture (UCM), remain consistently low in sediments predating ~1915 (Figure 2a–c) and gradually increase over the next 2 decades (Table 2). A dramatic increase (over 12-fold) in TSH levels follows, leading to a peak in the mid-1940s. A sharp decrease of TSH levels after the peak is followed by another dramatic increase leading to maximum TSH levels around the mid-1960s, after which fairly stable levels were found (Figure 2a).

Saturated hydrocarbons in sediments can originate from diverse inputs including higher plants, plankton, petroleum usage, and emissions from wood and coal burning. The distribution patterns of SH differ from source to source. Higher plant-derived SH are typically characterized by their low abundance of UCM and “preference” of odd- to even-numbered straight alkanes with a carbon preference index (CPI) value greater than 5 (3, 21). The absence of UCM and HMW fractions, together with abundant LMW alkanes (e.g., *n*-C_{15}, *n*-C_{17}, *n*-C_{19}, pristane) are major features of planktonic biomass. The petroleum-related SH are generally characterized by the lack of odd to even carbon preference (CPI ~ 1) and the significant presence of UCM relative to normal alkanes. Wood and coal combustion,

especially of the higher rank bituminous coals which have been widely used in New York City in the last century (22), generally emit relatively limited amounts of alkanes without carbon preference and much lower abundance of UCM relative to motor vehicle emissions (14, 23).

The most distinct feature in the CPI temporal profile is the transition of values from ~4.5 to ~2 over a brief period of approximately a decade (from mid-1930s to mid-1940s based on ^{210}Pb dating), correlating with a dramatic increase in TSH levels (Figure 2b). The CPI remains around 2 until 1980, followed by considerable variation toward the present, suggesting that the dominant *n*-alkane source varies between higher plants and petroleum. The generally inverse trends of total normal alkanes (TNA) and CPI (Figure 2b) support an association of elevated TNA with increased petroleum usage since the mid-1930s. The relative contributions of *n*-alkanes derived from petroleum and *n*-alkanes derived from higher plants can be calculated from a simple mass balance, assuming that no significant alterations in normal alkane distributions occur from sources to sediments. CPI ratios for higher plant and petroleum-derived *n*-alkanes are distinct (CPI from higher plants are ~6 and the ratio from petroleum is ~1). The calculated levels of petroleum-derived *n*-alkanes (Table 2) have a significantly strong correlation ($r^2 = 0.71$, $n = 17$, $p < 0.001$) with the concentrations of UCM (Table 2), which is mostly derived from petroleum biodegradation. However, the calculated levels of higher plant-derived alkane correlate poorly ($r^2 = 0.13$) with UCM concentrations, demonstrating that CPI is also useful for distinguishing between petroleum usage and higher plant sources of SH.

LMW alkanes (*n*-C_{15}–C_{20}), especially *n*-C_{17}, which is abundant in this core (unpublished data), are largely from planktonic algae, whereas HMW (*n*-C_{21}–C_{31}) alkanes with elevated CPI values are mostly associated with vascular plants. Therefore, the ratio of LMW/HMW can be applied as an indicator to assess the relative contributions of these two sources (24). LMW/HMW has an unusually high ratio in the top section, indicating relatively enhanced contributions of algae or other plankton in the lake in the last several years or a more rapid in situ degradation of LMW alkanes compared to relatively resilient vascular-derived HMW alkanes (3), producing a relative depletion of LMW alkanes in deeper core sections. The fact that regular applications of the algicide $CuSO_4$ to the lake ended in the 1970s, as reflected in the profile of Cu levels in the sediments (Chillrud, unpublished data), is consistent with the timing of the significant recent increase in the relative contribution of algal-derived alkanes.

The ratio of unresolved to resolved compounds (U/R) in the aliphatic fraction is commonly used as a diagnostic indicator of petroleum usage. A value >4 in the ratio U/R in aerosols indicates petroleum-related residues (25). U/R ratios were similar (2.9–3.3) in four coal smoke samples ranging in rank from lignite to bituminous (14). In conifer smokes, U/R ratios were observed ranging from 0.6 to 1.4 (26). In contrast, emissions from catalyst-equipped automobile engines and heavy duty diesel truck engines gave U/R ratios of approximately 5.5 and 9.3 respectively (21). In core CPF, the U/R ratio varies from 0.1 to 20, maintaining low levels (<2) before ~1910, followed by a significant first-order increase (~190-fold) over the next 3 decades (Table 2). EIA data indicates that petroleum use increased sharply around 1915 in the U.S. (18), consistent with the timing in the CPF core. It should be noted that the samples immediately above and below 38–40 cm were not analyzed for SH and PAHs. Consequently, the timing of the sharp increase in SH and PAH levels could be off by a few years. Nonetheless, the petroleum history together with the sharp increase in the U/R ratio provides an important consistency check of the ^{137}Cs/^{210}Pb dating models in the deeper sections of the core. Both of these radionuclides provide much tighter constraints on the top half of the core than on the deeper, older sections; ^{137}Cs provides only extrapolated dates in the deeper sections, while the counting errors on excess ^{210}Pb are much larger in the deeper sections, thereby allowing multiple age models.

The dramatic increase in U/R ratios, TSH, and TNA, and the decrease in CPI ratios from the 1910s to the 1940s (Figure 2a–c) indicate enhanced SH inputs from petroleum usage relative to other SH contributors, such as higher plants, algae, and wood and coal combustion. It should be noted that SH-associated petroleum inputs can include both petrogenic (direct petroleum release, e.g., crankcase oil leakage, oil spills) and pyrogenic sources (petroleum combustion, e.g., motor vehicle emissions), which are difficult to distinguish based solely on SH indicators. The highest ratios of U/R (~20) appears around the mid-1940s and the mid-1960s with ratios from 12 to 16 between these time periods.

It is quite interesting that the increase in the U/R ratio at ~1915 greatly precedes the large increase in TSH and TNA and decline in CPI occurring in ~1935. The U/R ratio upsurge between 1910 and 1940 suggests the influence of a petroleum source since around the mid-1910s, however, the similar levels of other ratios suggest this petroleum source remained relatively minor with respect to other hydrocarbon sources until the industrialization preceding WWII.

Temporal Trends of PAH Indicators

Yunker et al. (8) have summarized diagnostic ratios for some PAH source indicators (Table 1). A ratio of Fl/(Fl + Py) of less than 0.4 is indicative of petrogenic sources, between 0.4 and 0.5 of petroleum combustion-derived inputs, and greater than 0.5 of coal or wood combustion (8). Ratios of Fl/(Fl + Py) are higher than 0.44 throughout core CPF, indicating dominantly pyrogenic PAH sources. Despite their considerable variations, ratios of $C0/(C0 + C1)_{F/P}$ and $C0/(C0 + C1)_{P/A}$ are both greater than 0.5 throughout core CPF, also suggesting pyrogenic PAH sources (Figure 2g). Furthermore, parental PAHs dominate throughout the core (Figure 2h), indicating that combustion sources have been the dominant PAH sources into CP Lake since the late 19th century. Although there is a potential pathway for petrogenic inputs into CP Lake via runoff from the local park roads, Chillrud et al. (16) found that runoff from the local roads was not important for metal inputs relative to atmospheric inputs based on whole-core inventories of radionuclides and contaminant metals. The similarities between radionuclide-normalized, whole-core, contaminant metal inventories derived from the lake sediment core and that of soil cores collected from several locations in the park suggested that CP Lake sediments primarily reflected atmospheric inputs of these metals with little direct inputs of local road runoff. Since this comparison included Pb and Cd, two metals known to be highly elevated in road runoff and also strongly absorbed onto soil particles, it should also apply to leakage of fuel, crankcase oil, and lubricating oils, which also can be important in road runoff.

Although the correlation between parental PAH and the ratios of Fl/(Fl + Py), $C0/(C0 + C1)_{F/P}$, and $C0/(C0 + C1)_{P/A}$ suggest a predominantly pyrogenic PAH source for much of the history of deposition, ratios of A/(Pa + A) and BaA/(BaA + Chy) in three bottom samples (~0.04 and ~0.27) are lower than would be expected for combustion (Table 1), suggesting a petrogenic source (Figure 2f). According to the EIA report (18), petroleum was not used widely in the U.S. prior to 1900; thus, the most likely petrogenic source is fresh coal, which typically contains abundant alkyl PAHs (27). This petrogenic signal of the late 1800s is not apparent in the levels of parental PAHs (Figure 2g,h), which, as mentioned previously, indicate that combustion was the dominant PAH source throughout the core. Consequently, we attribute this discrepancy to the differential photolytic breakdown of the compounds in these isomer ratios. Previous work has shown that A and BaA have a much higher potential for photolysis than Pa and Chy, respectively; hence, the applicability of the molecular indicators A/(Pa + A) and BaA/(BaA + Chy) in “weathered” PAHs may be questionable (8).

Temporal profiles of 1,7/(1,7 + 2,6)-DMP and Ret/(Ret + Chy) are shown in Figure 2 and can be used as a "fingerprint" of softwood (e.g. fir and pine) combustion. A ratio of 1,7/(1,7 + 2,6)-DMP ranging from ~0.71 to ~0.91 was observed in emissions from softwood combustion (11, 28), ~0.43 from motor vehicle exhaust (29), ~0.63 in emissions from brown-coal-fired residential stoves (30), and around 0.67 in sub-bituminous and bituminous coal smoke (Simoneit, personal correspondence). Although elevated 1,7/(1,7 + 2,6)-DMP ratios (0.75–0.91) can be observed in fresh bituminous coal (27) and brown-coal smoke (Simoneit, personal correspondence), the distribution patterns of dimethylphenanthrene isomers (DMPs) from these fresh coals and sub-bituminous and bituminous coal-generated smokes differ from those in softwood combustion. 1,7-DMP occurs at a level comparable to related isomers such as 1,6-DMP in bituminous sources (27) (Simoneit, personal correspondence) and at levels overwhelmingly higher than 1,6-DMP in softwood combustion emissions (11). Retene is also preferentially produced in emissions from softwood combustion (7, 28); however, retene is also observed in fresh coal (27), diesel fuel and exhaust emissions from heavy-duty diesel fuels (31), and bituminous coal emissions (14), although at a low abundance relative to principal compounds (e.g. Fl, Py, BaA, Chy).

The ratio of retene to chrysene may have the potential to identify softwood combustion. Table 1 illustrates Ret/(Ret + Chy) ratios in different sources. Softwood combustion products have a value of 0.83–0.96 with a ratio of 0.96 in pine-burning emissions and 0.83 for balsam fir (28), whereas diesel engine emissions have values ranging from 0.05 to 0.5 (31). The ratio varies substantially in four coal smoke samples from approximately 0.5 in lignite and sub-bituminous (14) to <0.17 in brown coal and bituminous emissions (Simoneit, personal correspondence). The decreasing trends of the two softwood "fingerprints" in core CPF from the 1880s to the 1940s indicate that wood burning during this period had declined relative to other energy sources in NYC. This is consistent with the U.S. energy usage trends in the EIA data (18).

In three bottom sections predating 1900, elevated ratios of Ret/(Ret + Chy) (0.55–0.82) together with a much higher abundance of 1,7-DMP than 2,6-DMP and 1,6-DMP (Figure 3) indicate a strong softwood combustion input. Softwood is thought to have been used largely when wood was the primary energy source over a century ago (18). The corresponding Fl/(Fl + Py) ratios in sediments prior to ~1900 range from 0.62 to 0.72, which are just above the range of reported values (0.46–0.55) in initial wood combustion source emissions (8 and references therein). Some studies have also shown similar high ratios in remote lakes (13, 32).

After 1900, 1,7/(1,7 + 2,6)-DMP and Fl/(Fl + Py) ratios decline gradually until the 1940s (Figure 2e). A similar decrease is also observed in some remote lake cores (32). Contrary to these gradual declining trends, the Ret/(Ret + Chy) ratio declines sharply in the early 1900s and then remains at a relatively low level from the 1910s to the present (Figure 2i). Despite the different rates of decline, temporal trends of both the DMP and Ret/(Ret + Chy) ratios suggest a decreasing contribution from softwood combustion through the early 1900s. During the same period, PAH concentrations increase rapidly (~31-fold) (Figure 2d), whereas SH and UCM levels remain low with CPI ratios around 5, all indicating a minor petroleum-related hydrocarbon source. An increase in hardwood combustion could lead to the reduction of 1,7/(1,7 + 2,6)-DMP and Ret/(Ret + Chy) ratios due to their relative lower ratios in hardwood combustion emissions than softwood (28, 29); however, the extremely rapid increase in PAH levels over just 15 years together with the fact that NYC population only increased by ~20% during this period suggests that conversion to hardwood burning cannot account for the hydrocarbon signatures preserved in core CPF. We attribute this rapid PAH increase to the combustion of coal for residential heating and industrial usage at this period. Relative to wood and petroleum combustion, coal combustion can produce a greater

yield of PAHs (over 20-fold) and a lesser amount of UCM per unit of fuel burned (14, 28). In addition, the ratios of several indicators [Fl/(Fl + Py), 1,7/2,6-DMP, Ret/(Ret + Chy)] are in the range of coal combustion.

From ~1915 until ~1935, the gradual decrease in 1,7/(1,7 + 2,6)-DMP ratios (Figure 2e) suggests a continuous reduction in coal and/or wood combustion. Ret/(Ret + Chy) remains low, indicating negligible contributions of softwood combustion. Thus, the decline in Fl/(Fl + Py) and 1,7/(1,7 + 2,6)-DMP ratios most likely resulted from either a decrease in coal combustion, a relative increase in petroleum combustion, or both. Additionally, the temporal profile of U/R exhibits a first-order increase in this period, indicating a continuous increase in petroleum combustion. The gradual enhancement in petroleum combustion from the 1910s to 1930s probably results from the rapid increase in the number of motor vehicles after the first automobile assembly line was put into operation in 1913 (data are available at www.aaca.org).

Low ratios of Ret/(Ret + Chy) post-1910 span both the coal-dominant era and the following period of rapid increases in petroleum combustion, demonstrating this ratio's lack of sensitivity to these two sources. The similar trends of 1,7/(1,7 + 2,6)-DMP and Fl/(Fl + Py) observed throughout core CPF (Figure 2e) were not expected. As shown in Table 1, ratios of 1,7/(1,7 + 2,6)-DMP vary considerably among different combustion sources. Temporal trends of the DMP ratio in the core are consistent with the history of softwood combustion, coal combustion, and motor vehicle usage discussed above. Although published Fl/(Fl + Py) data (8) suggest similar ratios (>0.5) for wood and coal combustion sources, our analyses of CPF suggest a higher ratio of Fl/(Fl + Py) from local wood combustion in the period ~1870–1900s (0.72) than from local coal combustion in the early 1900s (0.62).

From the 1930s to 1960s, the ratios of Fl/(Fl + Py), Ret/(Ret + Chy), and 1,7/2,6-DMP suggest that major PAH inputs to the lake are from combustion of petroleum and coal. In contrast to TSH, PAH levels do not peak in the mid-1940s and mid-1960s, suggesting that SH and PAH may have different major sources for CP Lake. From ~1935 to ~1944, SH levels increase 10-fold, whereas PAH levels remain relatively constant, suggesting that the rapid increase in SH levels is not likely to have been caused by an increase in motor vehicle emissions. One potential source of the SH is incineration of municipal solid waste (MSW). Elevated levels of Pb, Sn, and Zn observed in another CP Lake core (CPH) between the late 1930s and the mid-1960s have been attributed to MSW emissions prior to the advent of effective pollution controls (16). Given that the uncertainty in model-derived ages for depth sections from the 1930s and 1940s is approximately 10 years (Figure 1), the elevated levels of TSH and MSW-derived metals are temporally similar. On the basis of this correlation, emissions from MSW incinerators would appear to contain a high abundance of TSH and comparable PAHs relative to other combustion sources. Abundant UCM was observed in a study of emissions from waste incineration plants (33).

Although various molecular indicators implicate petroleum combustion as the dominant pyrogenic source for the lake since the 1970s, some subtle variations in molecular ratios are noteworthy: There are higher 1,7/(1,7 + 2,6)-DMP and Ret/(Ret + Chy) ratios in some periods (e.g. the late-1960s, late-1970s, and early-1990s) relative to others (Figure 2e,i). The higher ratio of 1,7/(1,7 + 2,6)-DMP indicates an increase in either coal or softwood combustion; however, the concurrent rise in the Ret/(Ret + Chy) ratio, which is only responsive to wood combustion, suggests that increased wood combustion is a likely cause. This theory is supported by the EIA data, which records a period of increased combustion of wood in the late 1970s in the U.S. (18).

Utility of Various SH and PAH Indicators

In core CPF, the inverse relationship between carbon preference index and total alkanes (Figure 2b) indicates the reliability of CPI as a tool for differentiating SH contributions of higher plants from combustion sources. The U/R ratio is a sensitive indicator for petroleum usage. Fl/(Fl + Py) and 1,7/(1,7 + 2,6)-DMP can be used to study the relative contributions of three major PAH combustion sources (softwood, coal, and petroleum), while the Ret/(Ret + Chy) can be used to distinguish softwood combustion source from other combustion sources. A/(Pa + A) and BaA/(BaA + Chy) are less sensitive to source differences; therefore, interpretations based on these two ratios should be made with caution. The remaining four ratios [$C0/(C0 + C1)_{P/A}$, $C0/(C0 + C1)_{F/P}$, Par/(Par + Alkyl), and Ring456/TPAH] are sensitive indicators for differentiating petrogenic and pyrogenic PAH sources, but additional studies are necessary to fully exploit their potential for pyrogenic PAH source apportionment.

Acknowledgments

Funding for this project was provided by the Hudson River Foundation (A90095), the National Science Foundation (A11063), and NIEHS Superfund Basic Research Program (ES07384). We also thank the Central Park Conservancy, Martin Stute, Edward Shuster, and Jennifer Butler for assistance in collecting samples in CP. B.R.T. Simoneit is specially thanked for his useful advice.

Literature Cited

1. Cook JW, Hewett CJ, Heiger I. The isolation of a cancer-producing hydrocarbon from coal tar. J Chem Soc. 1933; 135:395–405.
2. Abrajano, TA.; Yan, B.; O'Malley, VP. High-molecular weight petrogenic and pyrogenic hydrocarbons in aquatic environments. In: Lollar, BS., editor. Treatise on Geochemistry Vol Environmental Geochemistry. 2003. p. 475-510.
3. Gearing JN, Buckley DE, Smith JN. Hydrocarbon and metal contents in a sediment core from Halifax harbour: A chronology of contamination. Can J Fish Aquat Sci. 1991; 48:2344–2354.
4. Baek SO, Field RA, Goldstone ME, Kirk PW, Lester JN, Perry R. A review of atmospheric polycyclic aromatic hydrocarbons: Sources, fate and behavior. Water Air Soil Pollut. 1991; 60:279–300.
5. Wang Z, Fingas M, Page DS. Oil spill identification. J Chromatogr A. 1999; 843:369–411.
6. Gunster DG, Gillis CA, Bonnevie NL, Wenning RJ. Petroleum and hazardous chemical spills in Newark Bay, New Jersey, USA from 1982 to 1991. Environ Pollut. 1993; 82:245–253. [PubMed: 15091773]
7. LaFlamme RE, Hites RA. The global distribution of polycyclic aromatic hydrocarbons in recent sediments. Geochim Cosmochim Acta. 1978; 42:289–303.
8. Yunker MB, Macdonald RW, Brewer R, Mitchell RH, Goyette D, Sylvestre S. PAHs in the Fraser River basin: A critical appraisal of PAH ratios as indicators of PAH source and composting. Org Geochem. 2002; 33:489–515.
9. Yan B, Benedict L, Chaky DA, Bopp RF, Abrajano TA. Levels and patterns of PAH distribution in sediments from New York/New Jersey Harbor Complex. Northeast Geol Environ Sci. 2004; 26:113–122.
10. Lima AC, Eglinton TI, Reddy CM. High-resolution record of pyrogenic polycyclic aromatic hydrocarbons deposition during the 20th century. Environ Sci Technol. 2003; 37:53–61. [PubMed: 12542290]
11. Benner BA, Wise SA, Currie LA, Klouda GA, Klinedinst DB, Zweidinger RB, Stevens RK, Lewis CW. Distinguishing the contributions of residential wood combustion and mobile source emissions using relative concentrations of dimethylphenanthrene isomers. Environ Sci Technol. 1995; 29:2382–2389.
12. Ramdahl T. Retene—A molecular marker of wood combustion in ambient air. Nature. 1983; 306:580–582.

13. Yunker MB, Macdonald RW. Alkane and PAH prepositional history, sources and fluxes in sediments from the Fraser River Basin and Strait of Georgia, Canada. Org Geochem. 2003; 34:1429–1454.

14. Oros DR, Simoneit BRT. Identification and emission rates of molecular tracers in coal smoke particulate matter. Fuel. 2000; 79:515–536.

15. Westerholm R, Christensen A, Törnqvist M, Ehrenberg L, Rannug U, Sjögren M, Rafter J, Soontjens C, Almén J, Grägg K. Comparison of exhaust emissions from Swedish environmental classified diesel fuel (MK1) and European program on emissions, fuels and engine technologies (EPEFE) reference fuel: A chemical and biological characterization, with viewpoints on cancer risk. Environ Sci Technol. 2001; 35:1748–1754. [PubMed: 11355188]

16. Chillrud SN, Bopp RF, Simpson HJ, Ross JM, Shuster EL, Chaky DA, Walsh DC, Choy CC, Tolley LR, Yarme A. Twentieth century atmospheric metal fluxes into Central Park Lake, New York City. Environ Sci Technol. 1999; 33:657–662.

17. Chaky, D. PhD dissertation. Rensselaer Polytechnic Institute; Troy, NY: 2003. Polychlorinated biphenyls, polychlorinated dibenzo-p-dioxins and furans in the New York metropolitan area: Interpreting atmospheric deposition and sediment chronologies.

18. Energy Information Administration, Report DOE/EIA-03842001. 2001. EIA Annual Energy Review 2001.

19. Bopp RF, Simpson HJ, Olsen CR, Kostyk N. Polychlorinated biphenyls in sediments of the tidal Hudson River, New York. Environ Sci Technol. 1981; 15:210–216.

20. Yan, B. PhD dissertation. Rensselaer Polytechnic Institute; Troy, NY: 2004. PAH sources and depositional history in sediments from the lower Hudson River basin.

21. Eganhouse RP, Kaplan IR. Depositional history of recent sediments from San Pedro Shelf, California: Reconstruction using elemental abundance, isotopic composition and molecular markers. Mar Chem. 1988; 24:163–191.

22. Rod, SR.; Ayres, RU.; Small, M. Report to Hudson River Foundation, Grant No. 001-86A-3. May. 1989 Reconstruction of historical loadings of heavy metals and chlorinated hydrocarbon pesticides in the Hudson-Raritan Basin, 1880–1980.

23. Rogge WF, Hildemann LM, Mazurek MA, Cass GR. Sources of fine organic aerosol. 2. Noncatalyst and catalyst-equipped automobiles and heavy-duty diesel trucks. Environ Sci Technol. 1993; 27:636–651.

24. Gearing PG, Gearing JN, Lytle TF, Lytle JS. Hydrocarbons in Northeast Gulf of Mexico shelf sediments: A preliminary survey. Geochim Cosmochim Acta. 1976; 40:1005–1017.

25. Mazurek, MA.; Simoneit, BRT. Characterization of biogenic and petroleum derived organic matter in aerosols over remote, rural and urban areas. In: Keith, LH., editor. Identification and analysis of organic pollutants in air. Ann Arbor Science/Butterworth Publishers; Boston: 1984. p. 353-370.

26. Oros DR, Simoneit BRT. Identification and emission factors of molecular tracers in organic aerosols from biomass burning Part 1. Temperature climate conifers. Appl Geochem. 2001; 16:1513–1544.

27. Radke M, Willsch H, Leythaeuser D, Teichmüller M. Aromatic components of coal: Relation of distribution pattern to rank. Geochim Cosmochim Acta. 1982; 46:1831–1848.

28. Fine PM, Cass GR, Simoneit BRT. Chemical characterization of fine particle emissions from fireplace combustion of woods grown in the Northeastern United States. Environ Sci Technol. 2001; 35:2665–2675. [PubMed: 11452590]

29. Benner BA, Gordon GE, Wise SA. Mobile sources of atmospheric polycyclic aromatic hydrocarbons: A roadway tunnel study. Environ Sci Technol. 1989; 23:1269–1278.

30. Grimmer G, Jacob J, Dettbarn G, Naujack KW. Determination of polycyclic aromatic hydrocarbons, azaarenes and thiaarenes emitted from coal-fired residential furnaces by gas chromatography/mass spectrometry. Fresen Z Anal Chem. 1985; 332:595–602.

31. Sjögren M, Li H, Rannug U, Westerholm R. Multivariate analysis of exhaust emissions from heavy-duty diesel fuels. Environ Sci Technol. 1996; 30:38–49.

32. Fernandez P, Vilanova RM, Appleby P, Grimalt JO. The historical record of atmospheric pyrolytic pollution over Europe registered in the sedimentary PAH from remote mountain lakes. Environ Sci Technol. 2000; 34:1906–1913.

33. Jay K, Stieglitz L. Identification and quantification of volatile organic components in emissions of waste incineration plants. Chemosphere. 1995; 30:1249–1260.

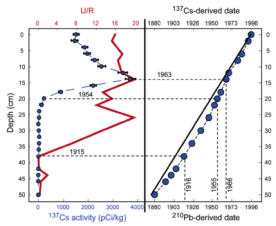

FIGURE 1.

Dating constraints provided by depth profiles of ^{137}Cs and the ratio U/R. Depositional ages estimated by a ^{210}Pb-derived constant mass accumulation model and a constant length accumulation model derived from ^{137}Cs are shown. Dashed lines follow the bottom scale; solid lines follow the top scale. All data are plotted at the top of the corresponding depth interval. Error bars indicate $\pm 1\sigma$ counting errors on radionuclide analyses.

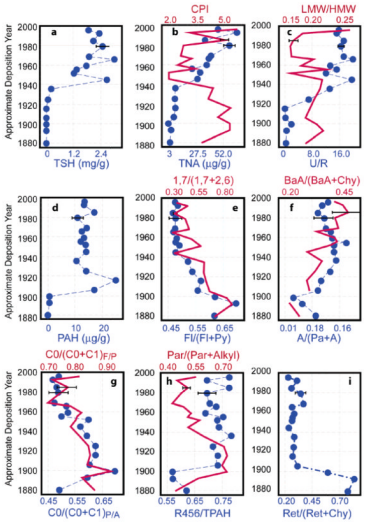

FIGURE 2.

Temporal profiles of various saturated and aromatic indicators (refer to Table 1 and text for definitions) in Central Park Lake core CPF. Trends indicated by solid lines (red) follow the top scale, and dotted lines (blue) follow the bottom scale. Error bars indicate ±1σ statistics. Representative error bars for the top scale are shown on the mid-1980s horizon; for the bottom scale, they are shown for the early 1980s horizon.

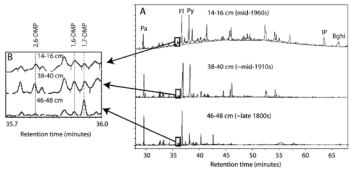

FIGURE 3.

(A) The chromatograms of aromatic fractions in three sections of core CPF. (B) Expanded-scale chromatograms highlighting the isomers of dimethylphenanthrene.

TABLE 1

PAH Source Indicators and Their Respective Diagnostic Ratios

ratios	description	petrogenic	petroleum burning	coal combustion	softwood combustion
Fl/(Fl + Py)[a]	the ratio of fluoranthene (Fl to PAHs with mass 202 (F1 plus pyrene (Py))	<0.40	0.40–0.50	>0.50	>0.50
A/(Pa + A)[a]	the ratio of anthracene (A) to PAHs with mass 178 [A and phenanthrene (Pa)]	<0.10	>0.10	>0.10	>0.10
BaA/(BaA + Chy)[a]	benzo[*a*]anthracene (BaA) divided by the sum of mass 228 [BaA + chrysene (Chy)]	<0.20	>0.35	>0.35	>0.35
$C0/(C0 + C1)_{P/A}$[a]	the ratio of parent PAHs with mass 178 (Pa, A) to PAHs with mass 178 (A; Pa) plus their C_1 alkyl homologues	<0.50	?	?	?
$C0/(C0 + C1)_{F/P}$[a]	similar calculation as above but with mass 202	<0.50	>0.50	>0.50	>0.50
IP/(IP + Bghi)[a]	the ratio of indeno[1,2,3-*cd*]pyrene (IP) to the sum of IP and benzo[*g*,*h*,*i*]perylene (Bghi)	<0.20	0.20–0.50	>0.50	>0.50
Par/(Par + Alkyl)[b]	the sum of the parent PAHs with masses 128, 178, 202, and 228 divided by these parent PAHs plus their related alkyl PAHs (C_1–C_4 Na; C_1–C_3P/A; C_1–C_2F/P; C1–BaA/Chy)	<0.30	>0.50	>0.50	>0.50
Ring456/TPAH[b]	the ratio of total 4–6 ring PAHs (mainly originated from combustion) to TPAHs	<0.40	>0.50	>0.50	>0.50
1,7/(1,7 + 2,6)[c]	the ratio of 1,7-dimethylphenanthrene (DMP) to 1,7-DMP and 2,6-DMP	?	0.40	0.65–0.68	0.90
U/R[d]	the ratio of unresolved complex mixture (UCM) to resolved hydrocarbons in saturated fraction	>4.0	>6.0	2.9–3.2	0.5–1.4
Ret/(Ret + Chy)	the ratio of retene (Ret) to retene plus chrysene	?	0.15–0.50	0.30–0.45	0.83 0.96

[a] From ref 8 and references therein.

[b] From ref 9.

[c] From ref 11.

[d] From ref 14. Diagnostic ratios of $C0/(C0 + C1)_{P/A}$ from combustion sources and ratios of 1,7/(1,7 + 2,6)-DMP and Ret/(Ret + Chy) from petrogenic sources are uncertain.

TABLE 2

Radionuclide Activities, SH and PAH Concentrations, and U/R Ratios in Core CPF

depth (cm)	dry mass (g)	^{137}Cs (Bq/kg)	±1σ	excess ^{210}Pb (Bq/kg)	±1σ	approx. date	TSH (μg/g)	UCM (μg/g)	U/R	HPDA[a] (μg/g)	PDA[b] (μg/g)	ΣPAH (μg/g)
0–2	5.82	57	4	213	20	1996	1840	1730	16.0	36	11	15
2–4	8.73	54	5	236	29	1992	2320	2170	15.3	23	41	14
6–8	9.89	73	5	190	20	1985	2060	1950	17.5	24	12	18
8–10	12.26	84	5	160	17	1980	2470	2330	16.6	17	40	12
12–14	13.02	126	7	96	15	1969	1880	1780	17.4	11	29	15
14–16	15.2	138	8	68	14	1966	2980	2840	20.1	14	24	14
18–20	16.83	33	3	67	14	1959	1760	1640	13.5	9	28	14
20–22	18.78	8	1	31	12	1955	1340	1260	15.3	10	14	13
22–24	17.18	4	3	57	23	1952	1210	1120	12.2	5	26	15
26–28	16.54	1	1	0	11	1945	2650	2530	19.9	5	24	15
30–32	23.08	0	1	5	9	1936	212	197	13.3	5	4	11
34–36	27.2	1	1	3	12	1925	76	67	7.04	5	4	15
38–40	21.19	0	1	NA[c]	NA	1916	8	1	0.10	7	3	27
42–44	24.04	0	1	NA	NA	1906	7	2	0.18	5	3	18
44–46	32.09	−1	1	−12	10	1899	10	7	1.95	2	1	1
46–48	32.01	−1	1	10	12	1893	9	4	0.62	4	2	1
50–52	32.48	−1	1	NA	NA	1880	7	2	0.38	2	3	0

[a] Higher plant-derived alkane calculated by CPI.

[b] Petroleum-derived alkane.

[c] Not analyzed; see text for definitions.